Thermochimica Acta 503–504 (2010) 40–45

Contents lists available at ScienceDirect

Thermochimica Acta

journal homepage: www.elsevier.com/locate/tca

Thermo-kinetics study of MIM thermal de-binding using TGA coupled with FTIR and mass spectrometry

Ijaz Ul Mohsin[a,*], Daniel Lager[b], Christian Gierl[a], Wolfgang Hohenauer[b], Herbert Danninger[a]

[a] Institute of Chemical Technologies and Analytics, Getreidemarkt 9, TU Vienna 1060, Austria
[b] Austrian Institute of Technology (AIT), Seibersdorf, Austria

ARTICLE INFO

Article history:
Received 13 November 2009
Received in revised form 8 March 2010
Accepted 9 March 2010
Available online 16 March 2010

Keywords:
MIM
De-binding
Modeling
Polymer decomposition
Thermo-kinetics
Mass spectrometry
FTIR spectrometry

ABSTRACT

The thermal de-binding of a metal injection molded (MIM) copper part was investigated at four different heating rates using a thermo-nanobalance coupled with infrared (FTIR) and mass spectrometry (MS), respectively. The FTIR and MS analysis have been employed to study the chemical reactions during thermal decomposition of the MIM polymeric binder. These techniques are effective for determining the thermal stability and product evolution as a function of temperature. The polymeric binder decomposition starts at approximately 250 °C yielding hydrocarbons in the C1–C6 range, with methane, ethylene, propylene, C4 and C5 composing the majority of gaseous products. The major decomposition reaction of polymeric binder was found to be autocatalytic. By using Netzsch thermo-kinetics software, a non-linear regression model was established. The predicted chemical reactions for the MIM thermal de-binding model were found to agree well with the calculated model curves.

1. Introduction

The MIM process is a manufacturing route for complex-shaped components that combines the shaping capability of polymer injection molding with the large material variety of metals and ceramics. It involves the mixing of metal powder with binder for viscous flow during mixing and molding. The binders used in metal injection molding are commonly mixtures of a polymer such as polyethylene or polypropylene, a synthetic or natural wax and stearic acid. After injection molding, which yields the "green" part, the wax is removed – e.g. by a solvent – in the so-called "de-binding" stage, while the polymer is retained as "backbone" to grant the required strength to the now "brown" part and is removed in the early stages of sintering. The thermal removal of the backbone components has been more critical in metal injection molding (MIM) because of long time needed to burn out the binders without introducing defects such as cracking, blistering and warping caused by emerging gases [1]. Thermogravimetric analysis (TG) has been widely used in studying pyrolysis phenomena. Methods for evaluation of mass loss curves obtained by this means have been studied [2,3]. The evaluation method which we employed is the simultaneous uses of Fourier transform infrared spectrometry (FTIR) and mass spectrometry (MS) with TG for the studies of polymeric binder. This approach allowed the simultaneous evaluation of bond breaking and product formation during decomposition of polymeric binder. Due to the ability to measure the simultaneous and continuous mass loss of materials and monitor the gaseous product, TG/FTIR and TG/MS techniques are widely employed in the material science field, including the study of pyrolysis, combustion, polymer degradation, evaluation of hazardous materials, and thermal stability of materials. Time or temperature-dependent gas evolution profiles can also be obtained from TG/FTIR and TG/MS techniques. There exist numerous studies in the past which investigated various aspect of de-polymerization [4,5]. These studies contained a wide range of experiments with varying techniques and conditions that examine the decomposition of different thermoplastics. All studies were focused on the final product after completed reaction. These techniques were used for the design of chemical decomposition reactions of MIM binder during the thermal de-binding. Thermal de-binding is a common method for the final removal of residual polymer from a MIM compact prior to sintering. This process is a combination of evaporation, liquid and gas migration, pyrolysis of polymer, and heat transfer in porous media.

The first part of the work was to demonstrate the usefulness of simultaneous use of TG-FTIR/MS for the polymeric MIM binder burnout, product formation and decomposition pathway. The second objective was to define the chemical reactions for each step that occurred during thermal de-binding of the copper MIM part.

* Corresponding author. Tel.: +43 1 58801 16159; fax: +43 1 58801 16199.
E-mail address: imohsin@mail.tuwien.ac.at (I.U. Mohsin).

0040-6031/$ – see front matter © 2010 Elsevier B.V. All rights reserved.
doi:10.1016/j.tca.2010.03.005

2. Experimental

The MIM sample was produced using a mixture containing 50 vol.% of pure copper from Ecka Granulate GmbH (MT-150) and 50 vol.% of binder. The examined samples were cut into shape with 3.5 mm × 3.5 mm × 6.0 mm dimensions. Solvent de-waxed samples were used to study the mass loss behavior of MIM parts during thermal removal of the backbone component using Netzsch TG 449 F1 Jupiter Thermo-Nanobalance coupled with infrared spectrometer (FTIR Bruker Tensor series 27) and mass spectrometer (QMS 403C Netzsch), respectively. The quartz glass transfer lines (diameter of 75 μm) leading to MS and teflon transfer line leading to FTIR were heated to 230 and 200 °C, respectively, to ensure that the entire sample entered the MS and FTIR in gas phase, i.e. to avoid condensation losses. The MS bargraph scans, which monitors *m*/*e* ratios from 1 to 300 approximately at a scan rate of 5 scans/s, resolution 25 and threshold limit E^{-12} were employed to determine the *m*/*e* ratios resulting from the decomposition of binder. A mass spectrometer operating in the electron impact mode at 100 eV was used in order to have sufficiently intense signals and to obtain fragmentation information. The FTIR spectra of the gases evolved were acquired at 4 cm^{-1} resolution in the range 400–4000 cm^{-1}.

The TG system was equipped with a rhodium furnace, allowing measurements to be carried out between room temperature and 1650 °C. An alumina sample holder was employed for the measurements. All experimental runs were performed in a protective atmosphere mixed of forming gas (95% N_2 and 5% H_2 with impurities 2 ppm O_2 and 5 ppm water contents) and argon (impurities 2 ppm O_2 and 3 ppm water contents) with gas flow of 50 and 120 ml/min, respectively (FG/argon ratio 1:2.4). Measurements were carried out from room temperature to 500 °C at four different heating rates, 0.5, 1.0, 1.5 and 2.0 K/min. To correct the influences of the measurement system, the reference spectra of MS, FTIR and baseline or calibration runs were carried out under the same conditions as used for the samples.

3. Results and discussion

During the thermal analysis different decomposition steps, which correspond to different mass loss rates, were obtained on thermal curves as shown in Fig. 1. The weight loss was slightly depending on the heating rate; therefore, the weight losses TG with DTA signals are shown in Fig. 2 for the heating rate (1.5 K/min). Gases were collected continuously during the decomposition steps and then analyzed through FTIR and mass spectrometry, simultaneously.

The first two onset DTA signals at 120.3 and 146.3 °C indicated the melting points of two components of MIM polymeric binder, respectively. The DTA signals corresponding to the mass losses were studied by FTIR and MS spectrometry. Fig. 3 shows the selected *m*/*e* ratio of products for the MIM copper parts at first mass loss (0.16%) of the thermal de-binding step. The *m*/*e* = 2, 14, 20, 28, 40 indicate the atmosphere components (mix of hydrogen, nitrogen and argon gases) which were used during the thermal de-binding process. The carrier gases *m*/*e* ratio observed throughout the MS spectrum is slightly unstable because of the gas flow rate fluctuation found during the process (flow rate control device shows some fluctuation). The *m*/*e* = 17, 18 shows the maximum evolution of water vapor at 230 °C which indicates the reduction of copper oxide to pure copper (0.4–0.5% oxygen content of pure copper powder). Copper oxides can be present in both stable oxidation states such as Cu_2O (Cu^{+1}) and CuO (Cu^{+2}), in red and black color, respectively. It is reported for micrometric powders that the reduction of Cu_2O by pure hydrogen is detected at ~150 °C and with a gas mixture reduction is achieved at ~250 °C [6]. Also a literature study [7] shows that CuO reduces to metallic Cu at ~200 °C under a 5% H_2/95% He gas mixture and Cu_2O under a flow of 5% H_2/95% He. It was shown that the oxide starts to be reduced near ~300 °C and that reduction of CuO is easier than the reduction of Cu_2O to copper. The color of Cu powder was brick red, most probable; the most oxides present at the surface are Cu_2O which are reduced close to the temperature found in the literature studies. The surface copper oxides were reduced by hydrogen and the resulting copper metal is catalytically active, playing the role as a catalyst during the reaction. It was found that the reduction of copper oxide by hydrogen gas was an autocatalytic consecutive reaction and takes place mainly at a copper–copper oxide interface (copper being the auto-catalyst) [8].

Reduction of the metallic oxide is described by the following reaction equations (1) and (2):

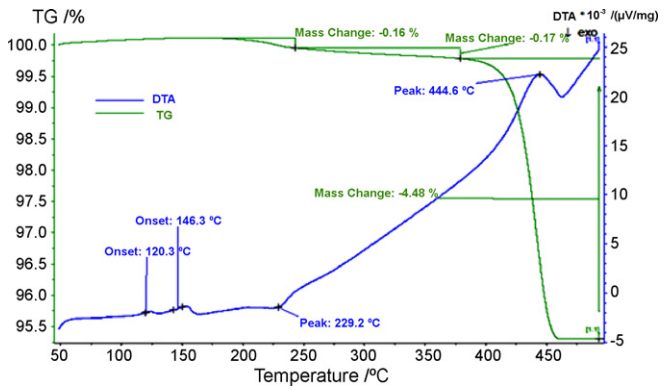

Fig. 2. TGA–DTA curves of solvent de-binded MIM copper part with heating rate of 1.5 K/min under forming gas/argon.

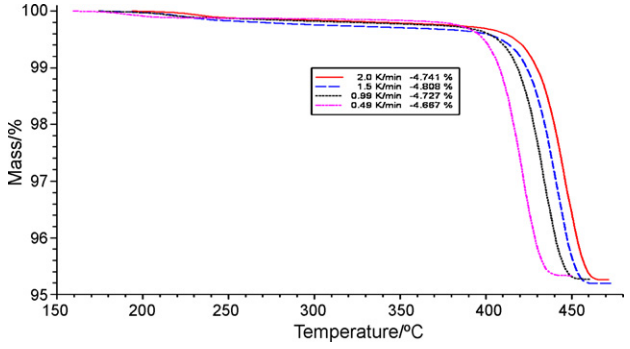

Fig. 1. TGA curves of MIM copper parts taken at different heating rates in a forming gas–argon mix.

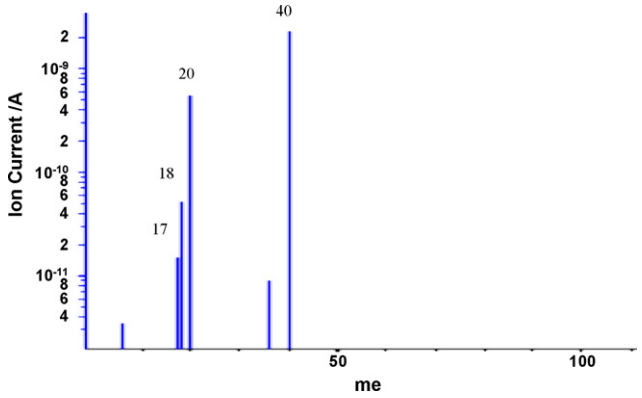

Fig. 3. MS bargraph obtained at the temperature (230 °C) of maximum decomposition rate for the evolution products for MIM copper during 1st step.

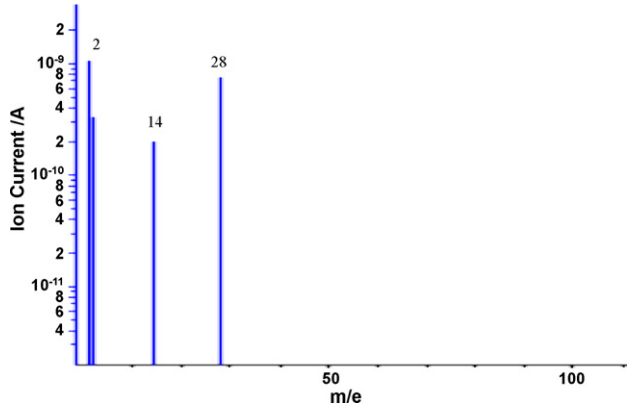

Fig. 4. MS bargraph obtained at the temperature (350 °C) of maximum decomposition rate for the evolution products for MIM copper during 2nd step.

$$CuO(solid) + H_2(gas) \rightarrow Cu(solid) + H_2O(gas) \quad (1)$$

$$Cu_2O(solid) + H_2(gas) \rightarrow Cu(solid) + H_2O(gas) \quad (2)$$

Fig. 4 shows the *m*/*e* ratio of products for 2nd mass loss (0.17%) of the thermal de-binding step at temperature 350 °C. The *m*/*e* = 2, 14, 28 indicate the evolution of carrier gases. It means that the gases evolved during this step cannot be seen in the mass spectrum (*m*/*e* more than 300). It could also be possible that the additives that are liberated in this temperature range condense in the transfer lines, which are kept at 230 and 200 °C. This step leads to decomposition of some antioxidants or stabilizers which are usually added to polymers to stabilize the polymer during processing and provides long term thermal stability by preventing thermo-oxidative degradation. It was confirmed by taking ATR (attenuated total reflection) spectra of each binder component (Fig. 5) separately. The circle stretching frequencies showed the presence of carbonyl (Fig. 5a)

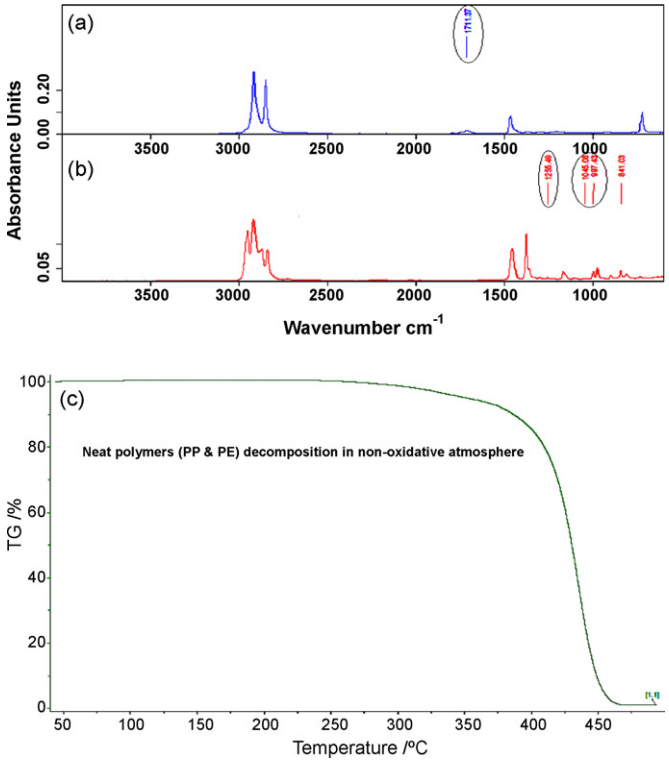

Fig. 5. ATR spectra of MIM polymeric binder, first (a) component of binder and second (b) component of binder. (c) The thermal decomposition TG curve of neat polymers mixer under non-oxidative atmosphere with heating rate of 1.5 K/min.

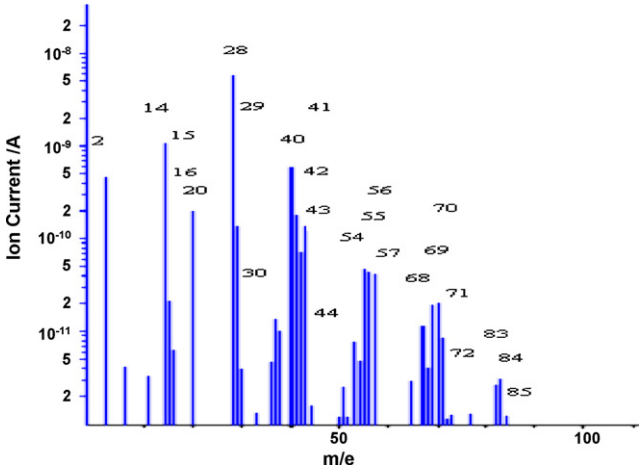

Fig. 6. MS bargraph obtained at the temperature (450 °C) of maximum decomposition rate for the evolution products for MIM copper during 3rd step.

and phosphorous (Fig. 5b) type antioxidants, respectively [9]. The stabilizers or antioxidants are mostly blends of organophosphate (phosphorous stretching) with molecular weight 646.9 g/mol and phenol (carbonyl stretching) with molecular weight 1178 g/mol [10]. In the recommended applications, these provide significant benefits, such as maintenance of original melt flow, low color formation, long term thermal stability. In polyolefins, the concentration levels for antioxidants range between 0.1% and 1%, depending on substrate and processing conditions. The decomposition temperature of such antioxidants or stabilizers start below 400 °C and the *m*/*e* ratio of even the decomposed components of these antioxidants or stabilizers are more than 300, i.e. cannot be seen in MS (1–300).

Fig. 6 shows the major pyrolyzed components of the polymeric binder. The polymeric binder was decomposed into hydrocarbon ranges from C1 to C6 and can be detected by the MS in accordance with experimental device setup presented in Table 1 below. Hydrocarbon molecular ions above *m*/*e* 100 are usually very weak, whereas fragment ions below *m*/*e* 100 are usually strong and detected in MS. It is also possible that high molecular ions could also be formed, but could condense in the transfer line and consequently could not arrive to the MS. The polymeric binder consists of more than one polymer so it was difficult to distinguish between fragmented components of each polymer, i.e. decomposed components can be the same for PP and PE, mostly hydrocarbons. The polymeric binder decomposed into heavier molecules which may itself be reactants and break further into small hydrocarbon chains by radical processes. The underlying chemistry, however, consists of thermolytic bond cleavage, recombination reactions, and volatilization of low molecular weight (MW) products. Copper does not have any catalytic effect or effecting the thermal decomposition of the polymeric binder. It was confirmed by experimental

Table 1
MS *m*/*e* peak assignments (pyrolysis products).

m/*e*	Possible species found in our experimental setup
85, 84, 83	$C_6H_{13}^+$, $C_6H_{12}^+$, $C_6H_{11}^+$
72, 71, 70, 69, 68	$C_5H_{12}^+$, $C_5H_{11}^+$, $C_5H_{10}^+$, $C_5H_9^+$, $C_5H_8^+$
58, 57, 56, 55, 54	$C_4H_{10}^+$, $C_4H_9^+$, $C_4H_8^+$, $C_4H_7^+$, $C_4H_6^+$
44, 43, 42, 41, 40	$C_3H_8^+$, $C_3H_7^+$, $C_3H_6^+$, $C_3H_5^+$, $C_3H_4^+$
30, 29	$C_2H_6^+$, $C_2H_5^+$
28	$C_2H_4^+$, N_2 (Carrier gas)
18, 17	H_2O, OH
16, 15	CH_4^+, CH_3^+
14	Nitrogen gas
2	Hydrogen gas

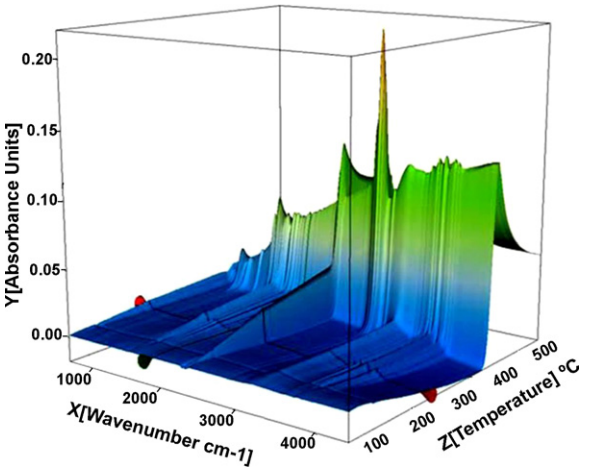

Fig. 7. 3D FTIR spectrum of the gases evolved during the thermal pyrolysis of the backbone binder.

run of neat polymer mixer (PP and PE) under the non-oxidative environment (Fig. 5c) as used for the other specimens.

Fig. 7 is the three-dimensional diagram (3D diagram) that provides a qualitative picture of the overall information obtainable from the TG/FTIR technique. In these diagrams the absorbance corresponding to the vibrational modes of the different bonds or functional groups is represented versus the wave number and temperature. Fig. 8 represents the corresponding IR data of the gaseous effluent with several prominent peaks, including 2959, 2924 cm^{-1}, representing $CH/CH_2/CH_3$ stretching, 1647 cm^{-1} C=C stretching, 1457 cm^{-1} CH_3 asymmetric bending, 1376 cm^{-1} CH_3 symmetrical bending, 887 cm^{-1} CH_3 rocking and C–C stretching. A summary of IR band assignments as found in the literature [11] is shown in Table 2.

It is noted that the CH, CH_2 and CH_3 symmetric stretching bands as well as CH_2 and CH_3 asymmetric stretching bands are all overlapping between 2850 and 3000 cm^{-1}. The peak in this region will be referred to as $CH/CH_2/CH_3$ stretching region. The characteristic gas phase CO_2 peak at 2360 cm^{-1} is attributable to air flow fluctuation found within the air vent inside the IR beam chamber (due to changes of the CO_2 content in the lab atmosphere) and in no way represents the polymer decomposition into carbon dioxide. The C=C stretching band is unique for olefins while the $CH/CH_2/CH_3$ stretching bands exists for both olefins and paraffins. No prominent stretching peaks were found for decomposed antioxidant fragments around 1710 cm^{-1} (carbonyl stretching) and 995–1050 cm^{-1} (O–P stretching) due to of too low concentration.

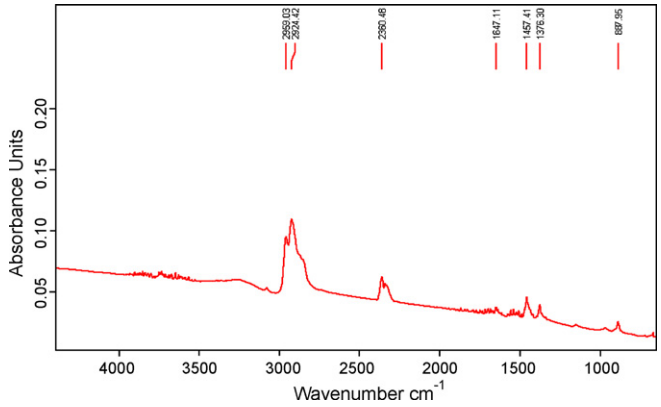

Fig. 8. FTIR spectra obtained at the temperature of maximum decomposition rate in the thermal pyrolysis of polymeric binder.

Table 2
Prominent IR band assignments.

Wave numbers	Assignment
888	CH_3 r, C–C s
973	CH_3 r + C–C s
997	CH_3 r
1163	C–C s + C–H w CH_3 r
1372–1381	CH_3 sb
1453–1465	CH_3 ab
1661	C=C s
2858–2972	CH_2/CH_3 as, $CH/CH_2/CH_3$ s
2340–2375	CO_2

ab = asymmetrical bending.
as = asymmetrical stretching.
r = rocking.
s = stretching.
sb = symmetrical bending.
w = wagging.

From the IR results alone, it is difficult to determine at what point the polymer decomposes. However, the MS results provide a conclusive insight into the thermal stability of polymeric backbone binder. The MS results indicate that initial decomposition occurs between 240 and 250 °C.

The intensity of the C=C stretching band is quite small as compared to $CH/CH_2/CH_3$ stretching and also FTIR data corresponding to MS data indicate that the majority of the products stretching can be classified as paraffinic.

In addition to decomposition mechanism, radicals (*) can undergo intermolecular reactions by gaining a hydrogen (+H) to form a paraffin or by losing a hydrogen atom (−H) to form an olefin. Based on this study; one proposed pathway for the general degradation mechanism was present in Fig. 9a. Fig. 9b describing the decomposition of high hydrocarbon molecular ion, i.e. how a large molecule (C_6H_{14}) breaks down further into small hydrocarbons. The main chemical reaction found during thermal de-binding of MIM copper was an autocatalytic one. An autocatalytic reaction is a chemical reaction where a product also acts as catalyst or reactant [12]. In such a reaction the observed rate of the reaction is often found to increase with conversion. This chemical reaction was employed to explain main reaction of the thermo-kinetics model of copper MIM part for back bone burnout.

Considering the above discussion, it is concluded that the first step (reduction of copper) is an independent reaction and polymeric decomposition was started at 230 °C into antioxidants (stabilizers) and into other C1–C6 hydrocarbons so it means that competitive reactions were involved during the decomposition of the MIM binder. Pyrolysis is usually modeled with autocatalytic kinetics and with parallel reactions having varying activation energies [13]. Friedman analysis [14] for determining the activation energy and pre-exponent factors was used in the development of the model. Taking these findings into the account, a fit was attempted using Netzsch thermo-kinetics software [15] with model (1), where the autocatalysis *n*th-order (Cn), *n*th-order (Fn) and *n*th-order (Cn) reaction types were used for the 1st, 2nd and 3rd steps, respectively, as predicted through the chemical reactions described above. The rate equation (A) is used for each reaction steps.

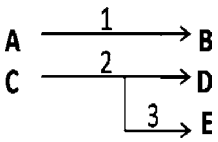

(1)

$$\frac{-d(a)}{dt} = Af(x)\exp\left(-\frac{E_A}{RT}\right) \quad \text{(A)}$$

where A is the pre-exponential factor, E_A specifies the activation energy, R is the gas constant, T is the temperature and $f(x)$

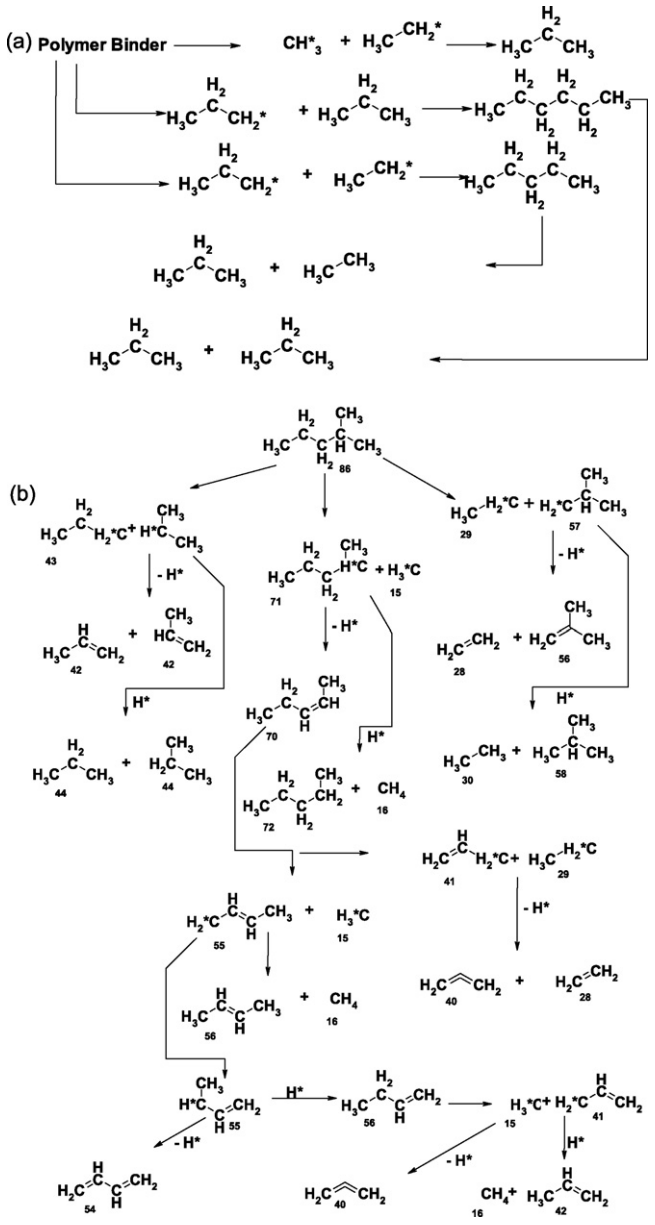

Fig. 9. (a) General degradation mechanism of polymeric binder under forming gas atmosphere. (b) The degradation mechanism of large hydrocarbon molecule ion into small fragments.

is reaction type. Reaction types used for each step are given below.

1. Cn–B = $e^n \cdot (1 + K_{cat} \cdot B)$, *n*th-order reaction with autocatalysis by the reactant B.
2. Fn = e^n, *n*th-order reaction.
3. Cn–E = $e^n \cdot (1 + K_{cat} \cdot E)$, *n*th-order reaction with autocatalysis by the reactant E.

With these reactions type model, an excellent fit was possible for all four measurements (correlation coefficient = 0.999760) and dependence of the total mass loss on the heating rate was conveyed correctly (Fig. 10).

The predicted chemical reactions for each step including Cu reduction, antioxidant and pyrolysis of backbone as well of the model were found to agree satisfactorily with the calculated model curves. The kinetics parameters obtained out of that proposed

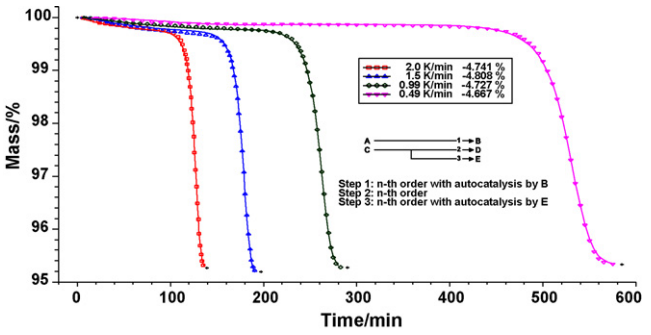

Fig. 10. Kinetic model analysis of the TG measurements at four different heating rates: experimental (dotted line) and simulated (solid line).

Table 3
Kinetic parameters.

Reaction step	Parameter	Optimum value
1	$\log A$ (s^{-1})	12.92
	E (kJ/mol)	224.09
2	$\log A$ (s^{-1})	12.70
	E (kJ/mol)	144.25
3	$\log A$ (s^{-1})	22.36
	E (kJ/mol)	264.99

Where $\log A$ (s^{-1}) = logarithm of the pre-exponential of reaction step and E (kJ/mol) = activation energy of reaction step.

Table 4
F-Test value.

Model code	*F*-Test value	Reaction type 1	Reaction type 2	Reaction type 3
t.i.c	1.00	CnB	Fn	CnE
t.i.c	1.63	CnB	CnD	CnE
t.i.c	1.98	CnB	CnD	A2
t.i.f	2.43	CnB	Fn	CnE

model, are presented in Table 3. The *F*-test values were also presented in Table 4 with comparison to other models, i.e. good fit quality.

The kinetic parameter obtained can be used for any kind of the copper feedstock sample dimensions and experimental runs. The kinetic parameters obtained, showed that the high activation energy is needed for decomposition of the backbone and copper reduction but stabilizers need less activation energy for the decomposition. If the apparent activation energy is greater than 220 kJ/mole, the decomposition reaction is autocatalytic [16].

The model enables to define temperature–time profiles for thermal de-binding that avoid blistering and cracks. The autocatalytic reactions, however, are not only accelerated by temperature but also by conversion and lead to sharp temperature increase during de-binding, so it is important to know reaction type, autocatalytic or not. Also partial mass loss versus time and temperature can be calculated.

4. Conclusions

The study confirms that combination of the complementary techniques TG/FTIR/MS provides a versatile analytical system for the detection and identification of gases evolved during thermal decomposition processes. The TG/FTIR/MS system makes it feasible to study reaction pathways for the formation of gaseous products and the degradation mechanisms of materials during pyrolysis. The polymeric backbone binder in a MIM "brown" Cu part was decomposed thermally into small hydrocarbon fragments. Using Netzsch thermo-kinetics software, a kinetic model was established. The pre-

dicted chemical reactions for the MIM thermal de-binding model were found to agree well with the calculated model curves. Model enables to optimize the process in order to save time, cost and defects.

Acknowledgements

This work was carried out within the project "TPM PIM" in Austrian Institute of Technology (AIT) Vienna. The first author is also thankful to Higher Education Commission (HEC) Govt. of Pakistan for financial support for PhD scholarship and to Prof. Simone Knaus for her great help in designing the degradation mechanism of backbone.

References

[1] R.M. German, Powder Injection Molding, Metal Powder Industries Federation, Princeton, NJ, 1990, pp. 321–346.
[2] W. Wendlandt, Thermal Analysis, 3rd ed., Wiley, New York, NY, 1986.
[3] Z. Petrovic, Z. Zavargo, J. Appl. Polym. Sci. 32 (1986) 4353–4367.
[4] W. Kaminsky, B. Schlesselmann, C. Simon, J. Anal. Appl. Pyrol. 32 (1995) 19.
[5] R.P. Lattimer, J. Anal. Appl. Pyrol. 31 (1995) 203.
[6] Y. Champion, F. Bernard, N. Millot, P. Perriat, Mater. Sci. Eng. A 360 (2003) 258–263.
[7] Y. Kim, J.A. Rodriguez, J.C. Hanson, A.I. Frenkel, P.L. Lee, J. Am. Chem. Soc. 125 (2003) 10684–10692.
[8] J. Słoczyński, R. Grabowski, A. Kozłowska, P.K. Olszewski, J. Stoch, Chem. Phys. 5 (2003) 4631–4640.
[9] E. Foldes, E. Maloschik, I. Kriston, P. Staniek, Polym. Degrad. Stab. 91 (2006) 479–487.
[10] http://www.ciba.com/, Product Name IRGANOX.
[11] S.A. Hedrick, S.S.C. Chuang, Thermochim. Acta 315 (1998) 159–168.
[12] V. Gold, K. Loening, P. Sehmi, Compendium of Chemical Terminology, IUPAC Recommendations, Blackwell Scientific Publications, Oxford, 1987, p. 34.
[13] J. Benjamin McCoy, Ind. Eng. Chem. Res. 38 (12) (1999) 4531–4537.
[14] J. Opfermann, J. Blumm, W. Emmerich, Thermochim. Acta 318 (1998) 213–220.
[15] J. Opfermann, E. Kaisersberger, Thermochim. Acta 203 (1992) 167–175.
[16] L. Bou-Diab, H. Fierz, J. Hazard. Mater. 93 (2002) 137–146.